Article

Microencapsulation of Lipases Produced by Dripping and Jet Break-Up for Biodiesel Production

Boris Guzmán-Martínez [1], Roberto Limas-Ballesteros [1,*], Jin An Wang [2], Liliana Alamilla-Beltrán [3], Lifang Chen [4,5,*] and Luis Enrique Noreña [5]

[1] Laboratorio de Investigación en Ingeniería Química Ambiental, ESIQIE, Instituto Politécnico Nacional, Col. Zacatenco, Mexico City C.P. 07738, Mexico

[2] Laboratorio de Catálisis y Materiales, ESIQIE, Instituto Politécnico Nacional, Col. Zacatenco, Mexico City C.P. 07738, Mexico

[3] Laboratorio de Microencapsulación: Interacciones, Estructura y Función, Escuela Nacional de Ciencias Biológicas, Instituto Politécnico Nacional, Av. Wilfrido Massieu S/N, Mexico City C.P. 07739, Mexico

[4] Departamento de Ingeniería Química Petrolera, ESIQIE, Instituto Politécnico Nacional, Col. Zacatenco, Mexico City C.P. 07738, Mexico

[5] Departamento de Ciencias Básicas, Universidad Autónoma Metropolitana-Azcapotzalco, Av. San Pablo 180, Col. Reynosa Tamaulipas, Mexico City C.P. 02200, Mexico

* Correspondence: rlimas@ipn.mx (R.L.-B.); lchen@ipn.mx (L.C.)

Abstract: A high-performance and scalable lipase immobilization method using a dipping and jet break-up technique was reported for the production of microcapsule biocatalysts with an entrapped cascade of lipase enzyme. The lipase from *Candida antarctica* (CALb) recombinant *Aspergillus oryzae* and from the vegetal of *Jatropha curcas* L. (var. Sevangel) in Morelos State of Mexico were entrapped by mixing with a sodium alginate biopolymer at different concentrations. The obtained microcapsules were hardened in a $CaCl_2$ solution, aiming at developing Ca^{2+} alginate microbeads with sizes mostly from 220 to 300 μm. The relationship between the process variables with the shape and size of the alginate drops before and after the gelation was established with aid of optical image analysis. The results showed that a critical Ohnesorge number (Oh) > 0.24 was required to form spherical microencapsulated beads. The biodiesel production via esterification/transesterification reaction was performed using the crude *Jatropha curcas* L. oil as feedstock in a batch reactor using lipase microcapsules as biocatalysts. Under the optimal reaction condition (ethanol-to-oil mass ratio: 10; water content 9.1 wt%, microencapsulated biocatalyst mass: 5.25 g, reaction temperature: 35 °C, pH of reaction mixture 7.5, stirring force 6 g), an approximately 95% fatty acid ethyl esters (FAEE) yield could be obtained. The biodiesel obtained from this work completely satisfied with the related ASTM D6751 and EN14214 standards. The microencapsulation technique reported herein allows the production of lipase microcapsules on a continuous large scale with the characteristics required for sustainable biofuel production and it can be also applied in other fields such as food processing and the pharmaceutical industry.

Keywords: biodiesel; transesterification; microencapsulated lipase; *Jatropha curcas* L. oil; biocatalysts

1. Introduction

Jatropha curcas L. is a 3–5 m tall perennial plant that belongs to the Euphorbeacea family [1]. This plant is widely distributed in the southern region of Mexico as it has a strong propagating ability and can grow under different environmental conditions even on wastelands and on gravelly, sandy, or saline soils [2]. The oil content of the crude *Jatropha curcas* L. seeds ranges from 30 to 50 wt%; and it even ranges from 45 to 60 wt% from kernels. Due to the presence of some anti-nutritional components, such as curcin and phorbol esters, the *Jatropha curcas* L. oil (JCLO) has been rendered unsafe for cooking. This nature makes it attractive as a non-edible vegetable feedstock for the oleo-chemical industries such as

fatty acids, soap, surfactants, detergents, and biodiesel production [3]. The JCLO is rich in unsaturated fatty acids including oleic (41.5–48.8%) and linoleic acids (34.6–44.4%) with a minor amount of saturated fatty acids such as palmitic (10.5–13.0%) and stearic acids (2.3–2.8%) [4].

As the present world is in a dilemma with the fast depletion of fossil fuels, a drastic need for developing alternative fuels such as biofuel arises. From an environmental point of view, biodiesel has great potential as a transportation vehicle fuel. JLCO merits as a feedstock for biodiesel production as it possesses low viscosity, good oxidation stability, low acidity, better cold properties, high cetane number, and low processing costs [5].

Different catalytic technologies have been applied for biodiesel production. The most commonly used catalysts in biodiesel production are homogeneous base catalysts such as KOH and NaOH [6,7]. However, homogeneous alkali processes exhibit some disadvantages such as the difficult recovery of the catalyst and environmental pollution. For this, heterogeneous catalysts including biocatalysts or enzymes have attracted great attention in the production of biofuels. A variety of techniques including immobilization of enzymes on proper support materials or matrix have been tensely investigated [8,9].

Mesoporous silica materials, for example, SBA-15, have been widely used as support for enzyme immobilization because of their well-ordered pore arrangement, large surface area, and abundant surface silanol groups [10]. However, only hydroxyls exist on the surface of these silica-based mesoporous solids as functional groups, and enzyme molecules are difficult to be stabilized on the SiO_2 surface via forming chemical bonds. Enzyme leaching may take place from these silica-based mesoporous biocatalysts during the reaction procedure.

It is noteworthy that natural biopolymers such as alginate, chitosan, and chitin have unique chemical-physical properties including non-toxicity, biodegradability, biocompatibility, and good harmony with proteins [11–13]. Particularly, these biopolymers contain various functional groups such as hydroxyls and carbonyl groups. Therefore, they can be used for lipase immobilization where direct reactions between the biopolymer matrix and lipase may occur, leading to the immobilization of lipase being more stable in comparison with silica-based mesoporous materials. Amongst the biopolymers, alginates have attracted special attraction because of their unique capacity for forming beads in the presence of divalent cations, such as calcium ions, in which lipases could be well immobilized [14].

Compared with traditional chemical catalysis, biodiesel production by lipase biocatalysts displays numerous advantages, such as minimal wastewater treatment and high catalytic selectivity [2–6]. Aiming at finding a suitable lipase with wide availability and high catalytic activity, researchers have screened various lipases for biodiesel production. Among these, lipase from *Candida antarctica* B showed promising results [7,15,16]. For lipase immobilization on nanomaterials, the entrapment of lipase in biopolymers such as sodium alginate is an interesting choice. This biopolymer is a naturally occurring polysaccharide which can be easily extracted from marine algae [17–19]. But lipase entrapped by vibrating, laminar jet break-up technology for the continuous production of microcapsules has not yet been reported.

In the present work, microencapsulation of lipase from *Candida antarctica* (CALb) recombinant *Aspergillus oryzae* and from vegetal of *Jatropha curcas* L. (var. Sevangel) was investigated by dripping and jet break-up of an aqueous mixture of sodium alginate at different concentrations. The obtained microcapsules were hardened in a solution of a Ca^{2+} salt with the aim of developing Ca-alginate microbeads with enough hardness and shape. These immobilized lipase microcapsules biocatalysts were employed for biodiesel production using the JCLO from the Tabasco State of Mexico as reaction feedstock. Ethanol, instead of methanol, was chosen as an acyl acceptor for the transesterification reaction with JCLO because the former is less toxic.

The microencapsulation technique reported herein not only allows for the production of lipase microcapsules on a continuous large scale with the characteristics required for sustainable biofuel production but also can be applied in other fields such as food processing

and the pharmaceutical industry. For example, the microencapsulated lipases are capable of catalyzing medicine synthetic reactions, such as anti-viral agent lamivudine, antibiotics, vitamins, anti-tumor, and anti-allergic compounds, etc. [20–22]. The immobilized lipases on silica were already applied for ester synthesis [23]. The wide applications in multiple fields of lipase microencapsulation technique via dripping and jet break-up way make it very attractive.

2. Materials and Methods

2.1. Materials

Lipase recombinant CALb (EC 3.1.1.3) (*Candida antarctica* B) of *Aspergillus oryzae* was obtained from Sigma-Aldrich (CAS: 9001-62-1, USA). Lipase of *Jatropha curcas* L. seeds of a nontoxic ecotype were obtained from the State of Morelos, Mexico.

Sodium alginate from brown algae (Sigma-Aldrich, CAS 9005-38-3, Lot # SLBZ2709) with medium viscosity ($\geq$2000 cP, 2%, 25 °C) was used in this experiment. Ethanol (GC grade), internal standard—ethyl decanoate, and GC-MS biodiesel standards (ethyl oleate, ethyl linoleate, ethyl palmitate, ethyl stearate) and triglycerides such as oleic acid, linoleic acid, palmitic acid, stearic acid were purchased from Sigma-Aldrich. Methanol (water content 0.02%) and ethanol (96%) were of commercial grade. Potassium hydroxide (99%) was purchased from Merck. All other reagents used in the experimental study were of analytical grade.

2.2. Crude Jatropha curcas L. Oil (JCLO)

The crude *Jatropha curcas* L. oil was procured from the local dealer at Huimanguillo, Tabasco State, Mexico. It was dried under vacuum at 120 °C for 4 h prior to its packing. In our laboratory, the crude JCLO was stored in tight containers at 15 °C and kept away from light in order to avoid any auto-oxidation. The different properties of crude JCLO were evaluated before the transesterification reactions. The resulting oil was filtered and directly used for the transesterification process. The fatty acid composition was determined by gas chromatography-mass spectrometry (GC-MS Torion T-9, PerkinElmer, American Fork, UT 84003, USA) (8700 Beverly Blvd, Los Angeles, CA 90048, USA). The iodine number was calculated using the standard test method for total iodine value (ASTM D1541).

2.3. Lipase Molecular Mass Measurement

The molecular mass of the purified lipase was determined by the matrix-assisted laser desorption ionization/time-of-flight mass spectrometry (MALDI-TOF-MS. Agilent, 8700 Beverly Blvd, Los Angeles, CA 90048, USA) technique on a Voyager DE-STR (Applied Biosystems) system equipped with a 337 nm nitrogen laser. The MALDI-TOF-MS spectra were acquired in the range of 10 to 45 kDa. Each analysis was performed in four replications. Five microliters of protein was mixed with 35 μL of freshly prepared sinapinic acid (15 mg/mL in 30% acetonitrile) and loaded onto the stainless steel MALDI plate and dried for 10 min at 37 °C.

2.4. Lipase Immobilization and Microcapsulation

The experimental system was set up in the Microencapsulated Laboratory— Structure and Function at the Instituto Politécnico Nacional. The equipment (BUCHI B390 Encapsulator) with different nozzles: 150:200, 200:350, and 250:500, was used for the synthesis of the microencapsulated lipase biocatalysts. Each lipase was immobilized by the entrapment technique through optimizing the concentration of lipase and sodium alginate. As an example, 1 g of lipase powder was dissolved in 1 mL of phosphate buffer (pH = 7.2) and added to 0.5 mL of glutaraldehyde solution under stirring for 3 h at 25 °C for cross-linking. Simultaneously, 15 g/L of alginate in water was prepared at 80 °C by stirring for 1 h, which was then cooled down to 35 °C. Afterwards, the cross-linked lipase was mixed with the sodium alginate solution and stirred for 15 min. This mixture was fed into the nozzle of the

vibrating jet system for encapsulation. When a drop of the lipase–alginate mixture hit the CaCl$_2$ solution (11 g/L) for hardening, the microspheres/microcapsules were formed.

The immobilized lipase beads were filtered, washed with a filter two times with 50 mM Tris-HCl buffer (pH 7.5), and then dried at room temperature under vacuum condition for 48 h. The amount of immobilized lipase was calculated by means of a mass balance method (Equation (1)).

$$P_a = (C_i V_i - C_f V_f)/W \tag{1}$$

where P_a is the amount of immobilized enzyme (mg/g) on the support; C_i and C_f are the initial concentration (mg/mL) in the solution and the final lipase concentration in the total filtrate, and V_i and V_f the volume of the initial lipase solution (mL) and the total volume of the filtrate, respectively; W is the weight of the microbeads (g). The measurement of the concentrations (C_i and C_f) was carried out using the Bradford method at 595 nm with a UV–vis spectrophotometer [24].

The density of the alginate solutions was measured using a specific gravity digital meter (Kyoto Electronics Manufacturing Co. Ltd., Kyoto, Japan). The viscosity of the solutions was determined using a viscometer according to the standard procedure (Model: LV-DV E203, Middleboro, MA, USA).

The surface tension of alginate solutions was determined under the following conditions: frequency, 1200 Hz; electrode, 1000 V; and pressure, 924 mbar. The formed beads were kept in the Ca^{2+} solution for 30 min at ambient temperature to promote the alginate cross-linking and bead hardening.

2.5. Characterization of Lipase Microcapsules

2.5.1. Sizing of Microcapsules by the Light Microscope

Samples were analyzed by using a Zeiss Axiovert 135 light microscope (Carl Zeiss S.P.A., Arese, MI, Italy) at ×320 and ×200 magnifications and a calibrated micrometer. About 50 microcapsules from each encapsulation trial were analyzed immediately after the process, during the storage at different conditions, and after each treatment described below.

2.5.2. Scanning Electron Microscopy (SEM) Analysis

Samples were analyzed with a scanning electron microscope (SEM-JEOL 2100, JEOL Ltd., Akishima, Tokyo 196-8558, Japan) to examine the surface morphology of microcapsules (MCs). The MCs were rinsed three times with MilliQ water (Lichrosolv Water for Chromatography) and then 10 µL of the sample was placed on a pin-type SEM specimen mount and maintained at 35 °C for 1 h in order to reach a gentle ethanolic dehydration of the microcapsules with 3% glutaraldehyde and post-fixed with 1% osmium tetraoxide. All samples were sputter-treated in a metallizer (Agar Sputter Coater) with gold–palladium to reach a coating thickness of 100 Å and then observed in high vacuum mode.

2.5.3. Confocal Laser Scanning Microscopy

The confocal microscopy images were analyzed using the ImageJ software (1.50I, imagej.nih.gov. Accessed on 12 March 2019). The hydrogel beads were studied by analyzing the average inside a single hydrogel bead using repeated scans. The ratio of pixel intensities of two images obtained from two wavelengths (488 nm and 543 nm) was calculated and correlated with the pH and temperature from the obtained standard curve. The images were processed by repeated scans with frame averaging from at least eight measurements.

2.5.4. Atomic Force Microscope (AFM) Analysis

The AFM instrument employed was a Nanoscope IIIa (Digital Instruments, Veeco Metrology Group), which was performed at a cantilever resonant frequency of around 277.5 kHz and a scan rate of 0.5 Hz with the tapping mode, using an etched silicon tip attached to the end of a cantilever (115–135 M in length). For the AFM analysis, the lipase beads were spread on a glass slide. The spring constant of the cantilever was in the range of 20–80 N/m.

2.6. Biodiesel Production and Experiment Optimization

The transesterification reactions of JCLO with ethanol were carried out in a 250 mL baffled flask (Corning, USA) placed in an orbital shaker (Heidolph, Germany). During the course of optimization studies, one parameter varied while keeping the others constant. For example, when the effect of temperature was studied, other parameters remained the same as: 10 g JCLO, ethanol to oil mass ratio 10, water content (relative to oil mass) 10 wt%, and 4.2 g microcapsules catalyst, pH value 7.5, and reaction time 24 h.

The flask reactor sealed with a rubber stopper and thermoplastic parafilm was shaken and heated in a water bath at various temperatures for 8–24 h. At the end of the reaction, the flask reactor was cooled to room temperature. The solid biocatalysts were separated from the bottom of the mixture by centrifugation at 4500 rpm for 20 min. After then, the product mixture was separated by a separation funnel where the upper layer corresponded to biodiesel (density 0.88 g/cm^3), the middle layer was related to the unreacted oil (density 0.91 g/cm^3) and the bottom was related to the byproducts (density 1.07 g/cm^3). The excess methanol in biodiesel liquid was evaporated at 85 °C under ambient pressure (at Mexico City the ambient pressure is approximately 0.88 atm). Once alcohol was removed, biodiesel was passed through an activated carbon column to remove impurities and then passed through a column of 4A molecular sieves to remove the moisture. The catalytic activity of the biocatalyst indicated as the biodiesel yield which was determined via the mass spectrometer-coupled gas chromatography (GC-MS, Torion T-9, PerkinElmer, American Fork, UT 84003, USA) method. Helium (99.99%) was used as a carrier to perform the chromatographic separation through an Elite-5 brand column with 5 m × 0.1 mm × 0.4 μm dimensions. The temperature of the injector and the detector was 270 °C and 250 °C, respectively. The column temperature was maintained at 270 °C.

The volume of biodiesel product was first measured and the volume yield was calculated according to the following Equation (2):

$$\text{Volume yield\%} = (\text{volume of product}/\text{volume of oil fed}) \times 100 \tag{2}$$

The fatty acid ethyl esters (FAEE) content in the produced biodiesel was identified using gas chromatography-mass spectrometry (GC-MS Torion T-9, Perkin Elmer, Waltham, MA, USA). This analysis technique also gives the distribution area for each component in the sample. The total biodiesel yield was finally calculated according to Equation (3):

$$\text{Biodiesel yield (\%)} = \text{FAEE percentage from GC analysis} \times \text{Volume yield} \tag{3}$$

2.7. Characterization of Biodiesel Products

2.7.1. FT-IR Characterization

The infrared spectra of biodiesel samples were obtained using an FTIR spectrometer (Perkin Elmer Spectrum 400, Waltham, MA, USA) in the wavenumber range of 4000–400 cm^{-1} with a 2 cm^{-1} resolution and 6 scans at room temperature.

2.7.2. Measurement of Physical and Chemical Properties

The physical and chemical properties of the biodiesel produced from JCLO, such as the pH value, specific gravity density, flash point, fire point, cloud point, viscosity, cetane number, acid value, free fatty acid value, saponification value, calorific value, moisture ash content, carbon residue, Na^+ and K^+ content, were analyzed at Unidad de Caracterización y Evaluación de Hidrocarburos (UCyEH) and the National Laboratory for Development and Quality Assurance of Biofuels of Mexico (LaNDACBio), the Mexican Centre for Cleaner Production (CMP + L), and the Center for Innovation in Inputs for Bioenergetics and Co-Products (CIBIOC). These properties were compared with American fuel standards (American Standard of Testing material, ASTM 6751–3) and European fuel standards (European Union Standard, EN 14214).

3. Results and Discussion

3.1. Biocatalysts Preparation

3.1.1. Lipase Microencapsulation

For the preparation of lipase microcapsules, a series of sodium alginate biopolymer solutions were used. The physical properties of the Na alginate solution varied with its concentration. As shown in Table 1, when the Na alginate concentration increased from 5 to 50 g/L, the density of the solution slightly increased, while the viscosity significantly enhanced by approximately 140.5 times. On the contrary, the superficial tension dropped by approximately 62.5%. The concentration of the sodium alginate solution also markedly impacted the critical Ohnesorge (Oh) number. A higher concentration of the sodium alginate solution led to a greater Oh value of the solution.

Table 1. Physical properties of different sodium alginate solutions.

Na$^+$ Alginate Concentration (g/L)	Density (kg/m^3)	Viscosity (mPa s)	Superficial Tension (mN/m)	Oh Number
5	995	37	72	0.073 to 0.094
15	1010	132	71	0.21 to 0.32
25	1014	568	67	1.0 to 1.6
35	1022	2800	56	5.5 to 6.4
50	1032	5200	45	10 to 16

In the present work, the experimental results showed that the minimum alginate concentration required for the formation of spherical microcapsules was 15 g/L, at which the critical Oh number was 0.24. It was also found that the viscosity of the Na alginate solution must be above a certain value, i.e., 60 mPa·s, in order to obtain spherical beads. When a drop of the mixture of crosslinked lipase with the alginate solution hits the CaCl$_2$ solution (11 g/L) for hardening, a competing force between the viscous surface tension force and the impact-drag force keeping the drop form arises, which affected the final formation of spherical beads. It was reported that as the lipase microcapsules were treated with CaCl$_2$ solution, the lipase activity, tolerance to alcohol, and stability were significantly enhanced [25]. These improvements are probably related to the incorporation of salt with the protein structure in lipase to form a more stable molecule that resisted the conformational change induced by alcohol in the transesterification reaction.

For the sodium alginate solution, as the Oh value was small, i.e., Oh < 0.20, the viscous and surface tension forces were lower than the minimum value for the formation of spherical beads. However, if the Oh value is too big, i.e., Oh > 5, some ovoid beads with polynuclear nuclei and irregular shapes, such as tear or pear-like shapes, could be formed. In the present work, the best Oh value was set between 0.21 and 0.32.

The diameter of the microcapsules depends greatly on the diameter of the internal/external nozzle of the encapsulation device and the flow rate of the mixture material. For the production of lipase microcapsules using alginate, a general rule of thumb is that the diameter of the microcapsules varied between 1.0 and 2.5 times the diameter of the inner nozzle of the device [26,27]. Increasing the flow rate resulted in capsules with larger diameters. In the present work, the average shell thickness of the microcapsules around 10 μm was selected as optimal since it has good ability to significantly control the beads output. The frequency of the system remained at an optimal value of 1092 Hz in order to avoid the formation of miniature-size satellites of beads. After the drops entered into the calcium ions solution, the mixture of crosslinked lipase with the alginate solution underwent conformational changes, giving rise to the well-known alginate gelation. This alginate gelation is based on the dimerization of the chain and, finally, on the greater aggregation of dimers.

3.1.2. Particle Size Distribution and Morphology of the Lipase Microcapsules

The size of microcapsules (MCs) was evaluated immediately after their production. The particle size distribution of the microencapsulated CALb-alginate is reported in Table 2. The MCs had an average diameter ($\pm$ standard deviation) of 240 $\pm$ 12 μm. Moreover, the MCs' size remained unchanged during their storage.

Table 2. Particle size distribution of microencapsulated CALb-alginate.

Aperture (Microns)	Class Weight Retained (%)
550	0
320	6.3
280	6.14
240	77.3
180	10.3
125	0

Figure 1 shows SEM micrographs and laser confocal microscopy images of MCs. Most MCs were perfectly spherical in shape with a continuous surface without hollow zones (Figure 1A). To investigate the lipase location within the microcapsules, the CALb tagged with alginate was incorporated in the aqueous phase. The green fluorescence image revealed the presence of the CALb, where a high density of CALb existed in the surface and wall of microcapsules and it was superimposed with the green fluorescence.
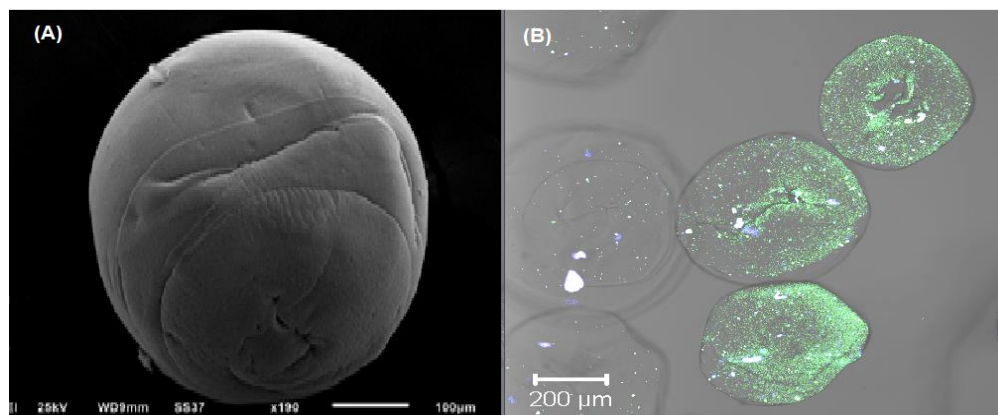

Figure 1. SEM and confocal images of alginate microcapsule beads with lipase (MC-CALb). (**A**) With a characteristic morphology at ×1000 magnification; (**B**) fluorescence microscopy images at ×400 magnification of CALb-alginate microcapsules.

Figure 2 shows SEM and AFM micrographs of the microcapsule beads composed of alginate CALb and vegetal lipase. They are believed to be a fair representation of the whole sample since they were chosen after a thorough analysis of a large number of specimens. The SEM micrographs confirmed the different morphological features and crystallite size. The samples showed a normal distribution with an arithmetic mean size of about 0.5–1 μm. The sample with CALb Lipase, Figure 2A, had many small crystallite sizes around 50–100 nm connected into a fiber-like morphology. The length of fibers was approximately 0.5–0.6 μm. For the sample with vegetal lipase, Figure 2B, the crystallite size was smaller and distributed along 30–60 nm; and all of them showed spherical shape. The morphology of these two samples was also observed by the AFM technique (Figure 2C,D). The immobilized enzyme with vegetal lipase sample had a relatively homogeneous particle size distribution; otherwise, the sample immobilized with alginate CALb showed a rough surface and an uneven particle size distribution.
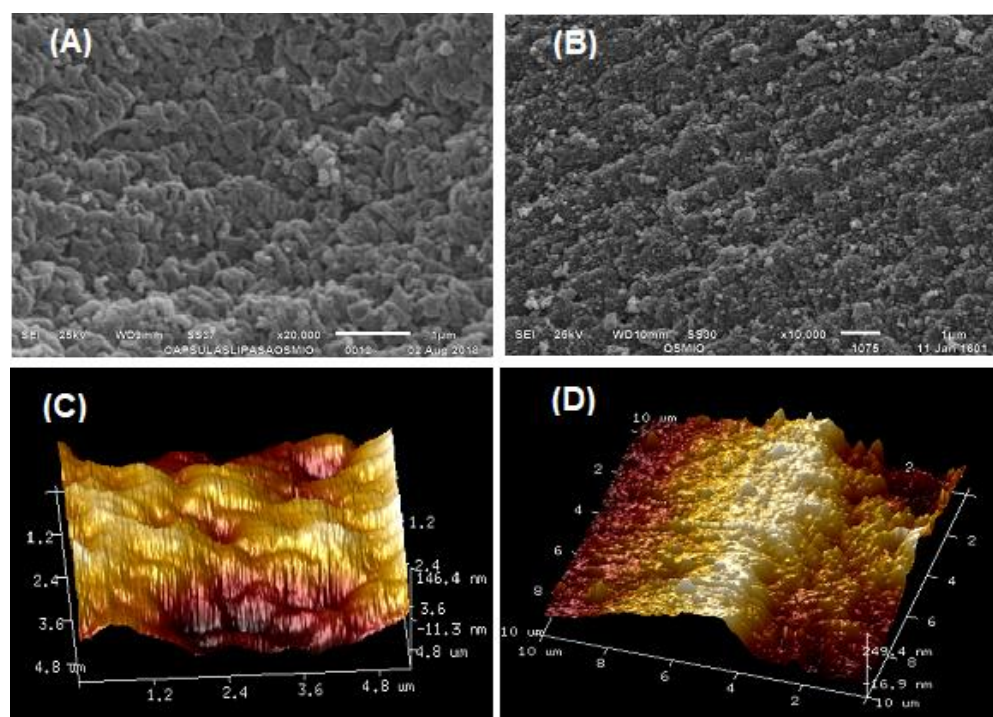
Figure 2. SEM images and three-dimensional AFM surface topology of samples. (**A**,**C**) are samples were with CALb lipase; (**B**,**D**) are samples were with vegetal lipase.

3.1.3. FT-IR Characterization of Immobilized Lipase CALb

In order to study the change of the lipase functional groups during the immobilization process, the FT-IR spectra of the immobilized lipase CALb were recorded. For comparison, the FT-IR spectra of alginate and alginate with sodium phosphate buffer are also presented (Figure 3). The strong and wide IR absorbance band centered at 3445 cm^{-1} in the region 3650–3100 cm^{-1} was attributed to the –OH species stretching vibration of adsorbed water and to the stretching vibration of the –NH bond in the protein structure in lipase [28]. These two bonds are overlapped in the same wavenumber region. The IR bands at 2927 and 2950 cm^{-1} which merged into the wide peak in 3650–3100 cm^{-1} as shoulders were assigned to the –CH$_2$ stretching vibration and to the –CH bending vibration linked with the protein structure in CALb lipase, respectively [28,29]. There is an intense IR signal at 1650–1550 cm^{-1} which was ascribed to the CALb secondary structure during the immobilization. The infrared signals observed in this region were assigned to the asymmetric stretching vibration of the carboxylated ion group $\upsilon(CO_2{}^-)$ and the asymmetric bending vibration of –N–H in amino acids in the protein structure of lipase [30,31]. This band indicated the attachment of protein molecules containing amino groups to the free aldehyde groups, resulting in the formation of covalent bonds with the alginate biopolymer network. The IR band at 1400 cm^{-1} was assigned to the extension vibration of –CH$_2$ groups in the hydrocarbon chain. The other IR signals at 1223 cm^{-1} and 1177 cm^{-1} were assigned to the vibration of the C–O bond corresponding to the methoxy group in carboxylated ion group bonds [32]. Because the IR spectrum of the immobilized CALb sample is almost identical to that obtained from the mixture of alginate and sodium phosphate buffer, demonstrating that the lipases had been well immobilized on the alginate network.
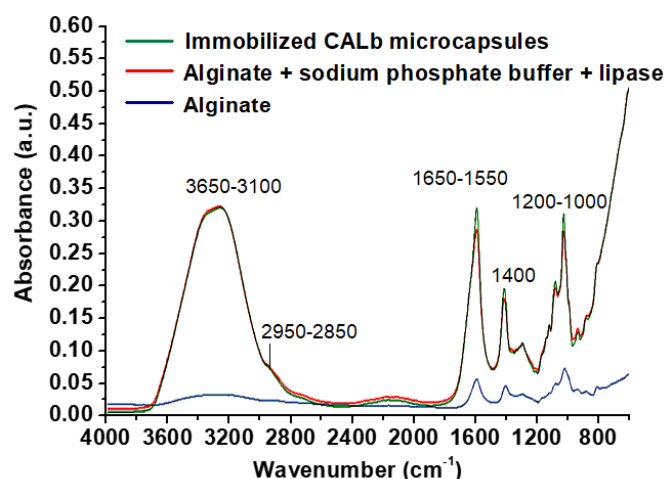
Figure 3. FTIR spectra of the Na alginate, mixture of alginate and sodium phosphate buffer, and immobilized CALb microcapsules.

3.2. Properties of Crude Jatropha Curcas L. Oil as Feedstock

The specific density of the crude JCLO was 0.91 g/cm^3. There was no significant difference with respect to the ASTM D6751 standards which establish the biodiesel-specific density within a range of 0.860 to 0.900 g/cm^3. The density of the JCLO feedstock is slightly higher, but it can be used for the present experiment for the transesterification reaction.

The properties of JCLO used for the present experiments are reported in Table 3. The viscosity of the crude JCLO falls in the range between 24.50 and 28.80 cSt. The ASTMD6751 standard indicates that the viscosity of biodiesel should be in a range of 1.9 to 6 cSt. Oils with viscosity values greater than this range cannot be directly used as engine fuels because they would accumulate impurities in the injector, causing operational problems. The viscosity value of the crude *J. Curcas* L. oil does not satisfy well the ASTMD6751 standard. Therefore, the higher viscosity of JCLO must be reduced via the catalytic transesterification process.

Table 3. Properties of crude *Jatropha curcas* L. oil.

Property (35 °C)	Crude *Jatropha curcas* Oil
Density (g/cm^{-3})	0.91
Viscosity (cSt)	24.50 to 28.80
Flash point (°C)	236
Moisture	0.15
Acidity index (KOHmg/g oil)	0.70 to 0.79
Iodine index (g I$_2$/100 g)	98.82 to 102.61
Peroxide index (meq/kg)	2.0 to 2.7

The acid number varied between 0.70 and 0.79 mg KOH/g. Oils having acidity greater than 4% need acidic esterification to decrease the percentage of free fatty acids, followed by an alkaline transesterification; while values lower than 1% are considered as optimal and transesterification can be performed directly. The crude JCLO in the present experiment showed less than 1% free fatty acids, indicating that previous treatment is not necessary.

The JCLO had an iodine index between 98.82 and 102.61 g/100 g. The iodine index is the average of the unsaturated fatty acids in the oil. When the iodine index is low (26 to 48 g/100 g), the oil is saturated and tends to solidify; when the iodine index increases (94 to 135 g/100 g), the level of unsaturation in the carbon chains increases, thus the oil remains liquid, but this affects the viscosity. The JCLO used for the present work showed a higher content of unsaturated fatty acids, a property that gives it better stability to prevent oxidation and a lower melting point, which would contribute to biodiesel having better flow characteristics in cold environments. Akbar et al. reported an iodine value

of 103.62 g/100 g in *Jatropha curcas* germ oil samples from regions of Malaysia [33]. The iodine values found in *Jatropha curcas* oils in Tabasco, Mexico, are similar to their report and are within the ASTM D6751 range (120 g/100 g) that establishes the permissible limits of biodiesel acceptability.

The GC analysis confirmed the presence of four groups of main fatty acids in the JCLO: oleic acid, linoleic acid, palmitic acid, and stearic acid. Table 4 shows the various fatty acids and the number of double bonds in the hydrocarbon chain. The saturated fatty acids consisted of lauric (C12: 0), myristic (C14: 0), palmitic (C16: 0), stearic (C18: 0), and arachidic (C28: 0); these represented approximately 19.54% of the total components. On the other hand, the unsaturated fatty acids were palmitoleic (C16: 1), oleic (C18: 1), linoleic (C18: 2), linolenic (C18: 3), and linolenic (C20: 1), of which oleic and linoleic acids formed approximately 80.02%; the rest of the unsaturated fatty acids constituted 1.16%. These values are consistent with the results reported by Gopale and Zunjarrao who claimed that in regions of India, the fatty acids showed higher content of oleic acid (41 to 49%) and linoleic acid (26 to 31%) [34].

Table 4. Fatty acids of the crude JCLO (Tabasco, Mexico).

Saturated Fatty Acid	Carbon Chain	Number of Double Bond	wt%
Palmitic acid	C16	0	11.17
Stearic acid	C18	0	8.06
Myristic acid	C14	0	0.12
Arachidic acid	C20	0	0.19
Monounsaturated fatty acids			
Palmitoleic acid	C16	1	0.46
Oleic acid	C18	1	44.80
Polyunsaturated Fatty Acids			
Linoleic acid	C18	2	35.22
linolenic acid	C18	2	0.70

The JCLO contained oleic (44 to 46%), stearic (3 to 8%), and myristic (0.1 to 0.4%) acids, and the acid number varied from 0.70 to 0.79 mg KOH/g. These data are quite similar to those reported by Martínez et. al., from samples from the state of Veracruz located in the south of Mexico, containing 41 to 42% oleic acid, 42 to 44% linoleic acid, 9 to 11% palmitic acid, 2 to 3% stearic acid, 0.3 to 0.4% myristic acid, and 0.3 to 0.4% of palmitoleic acid [35]. The free fatty acids that contribute to the acid number are one of the most important properties related to the oil quality. A high content of free fatty acids causes problems in the transesterification process. In our sample, the oil presented less than 1.1% of free fatty acids, indicating that does not require previous treatment.

3.3. Biodiesel Production via Jatropha curcas L. Oil Transesterification Reactions
3.3.1. Effect of Reaction Temperature

In the present work, for all the experiments, the reaction medium was justified at weak basic condition (pH = 7.5) and the ethanol to oil mass ratio was fixed at 10. The effects of other factors, such as reaction temperature, reaction time, water content, and immobilized free enzyme loading on the catalytic activity were investigated. Temperature influence was studied in the range of 25–50 °C and the FAEE yield results are shown in Figure 4. The optimum temperature for the transesterification reaction was found to be 35 °C. As the reaction temperature was further increased, a decrease in ethyl ester formation was noticed. This resulted from the partial deactivation of lipase at higher temperatures, similar to the report by Antczak et al. [36] and Fernandez-Lorente et al. [37]. Hence, biodiesel production at low temperatures using biocatalysts has an added advantage over the traditional heterogeneous catalysts, because it is environmentally friendly and is an energy-saving mode. In comparison with the immobilized vegetal lipase, the catalytic

activity of the recombinant immobilized microcapsule was more active under the same reaction condition.
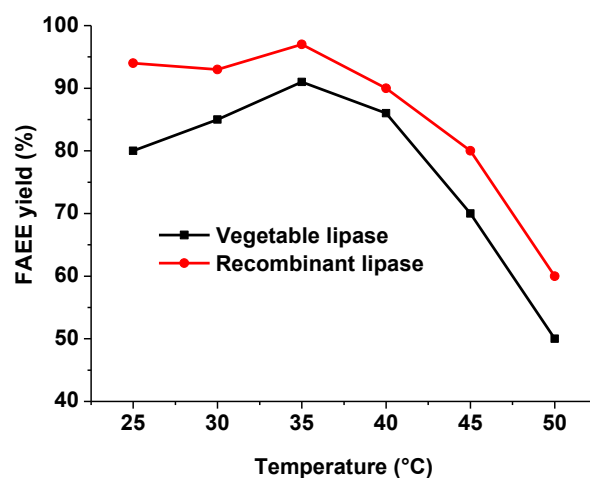

Figure 4. Effect of temperature on the transesterification of crude *Jatropha curcas* L. oil using immobilized lipase catalysts. Experimental parameters: Jatropha oil 10 g, ethanol to oil mass ratio 10, water 10 wt%, catalyst mass 4.2 g, mixing intensity 3 g RCF, pH value 7.5, and 24 h reaction time.

3.3.2. Effect of Water Content

Water content in the reaction feedstock produces an important effect on the transesterification reaction. Figure 5 showed a considerable increase in ethyl ester formation in the presence of a proper amount of water. As the water content was lower than 9.1 wt%, a promotion effect was observed. This results from the fact that a proper amount of water in the reaction mixture generates many micro water–oil interfaces on one hand, and helps to retain the 3D lipase structure on the other hand. Under agitation, water addition into oil provides numerous water–oil microdroplets with huge space at the interfaces. This may change the ionization condition of the enzyme, consequently, affecting the active conformation of lipase and the interaction between the enzyme and substrate. In the oil–water interfaces, lipase will convert into an open-lid conformation to allow substrates to access its active sites, and finally, the lipase catalytic activity can be initiated [15].
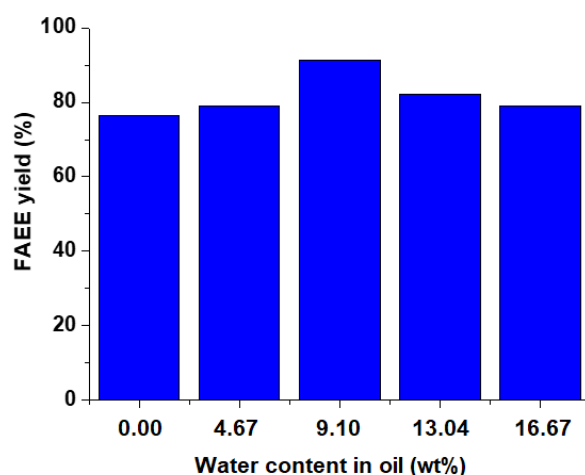

Figure 5. Effect of water content on immobilized lipase-catalyzed transesterification of crude *Jatropha curcas* L. oil. Experimental parameters: Jatropha oil mass: 10 g; oil to ethanol mass ratio: 1:10; immobilized lipase CALb mass: 4.2 g; reaction temperature: 35 °C; and reaction time: 24 h.

When the water content in the reaction mixture was 9.1 wt%, the ionizing environment may be suitable for the combination between enzyme and substrate and thus the

best catalytic activity was achieved. However, when the water content was greater than 9.1 wt%, a certain amount of hydrolyzed ester was generated via saponification reaction, inhibiting the catalytic activity to some extent. Hence, the optimum water content in the reaction mixture plays an important role in minimizing the hydrolysis and maximizing the transesterification activity of the immobilized lipase [38–40].

3.3.3. Effect of the Immobilized Enzyme Loading

The effect of the immobilized lipase catalyst mass on the transesterification of crude JCLO was studied in the range of 3~10 g with a constant ethanol-to-oil ratio of 10 and 9.1 wt% water in the reaction feedstock. The other reaction parameters remained the same. Here, 1 g lipase microencapsulated catalyst corresponds to 19.23 mg of immobilized enzyme. FAEE yield as a function of lipase immobilized amount in catalysts is shown in Figure 6. For both immobilized recombinant lipase and the immobilized vegetal lipases, a higher ethyl esters yield was obtained in the range between 80 and 120 mg free lipase, these corresponded to catalyst amount between 4.16 and 6.24 g. The activity of the immobilized recombinant lipase catalyst was greater in comparison with that of the immobilized vegetal lipase catalyst. We have determined the optimal catalyst mass of 5.25 g in the present experiment.
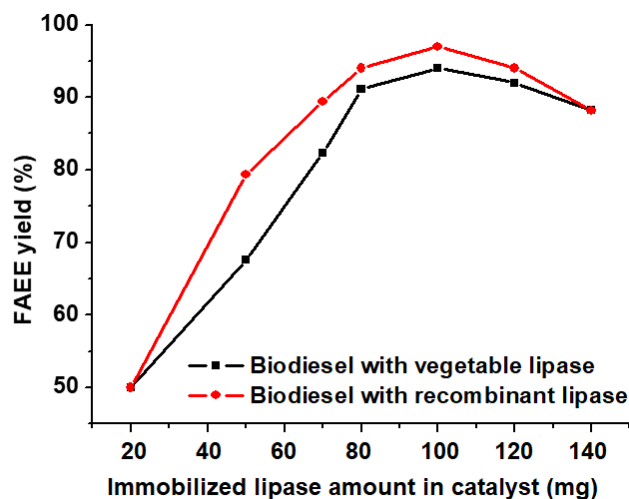

Figure 6. Effect of the immobilized lipase amount in microcapsules on FAEE yield. Experimental parameters: Jatropha oil mass: 10 g; ethanol to oil mass ratio: 10; water content: 9.1 wt%; reaction temperature: 35 °C; reaction time: 24 h, and pH value: 7.5.

There was a slight decrease in biodiesel yield at higher catalyst mass, which chiefly results from the molecular diffusion and mass transfer limitations within the immobilized lipase during the reaction [41,42]. Furthermore, a higher free enzyme concentration increases the acidity, because the enzyme usually can catalyze the hydrolysis reaction, increasing the production of fatty acids [43]. Severe hydration significantly affects the catalytic activity because the activity of the catalyst competes with water adsorption and/or hydrolysis on the active sites that impeded the direct contact between the active phases by the interposition. Therefore, the production of FAEE was initially dependent on the amount of the biocatalyst; but as the catalyst amount increased more, the product yield slightly decreased. Lipase was easily hydrated by the environment which leads to the enzyme hydration problem. The viscosity of the reaction medium was very sensitive to the temperature. At 35 °C, the viscosity can be reduced by approximately 25% relative to the cool beginning. Therefore, the catalyst was added to the reaction mixture at 35 °C, not at the cool beginning, which may increase the diffusion of reactants on the surface of catalysts and favor the surface reaction.

3.3.4. Effect of Reaction Time

The effect of reaction time on the transesterification reaction was studied up to 24 h under the optimal experimental condition. Biodiesel samples were taken every 1 h reaction interval and were analyzed by GC-MS technique. The obtained results are depicted in Figure 7. At the end of 1 h reaction, 45% of ethyl esters were produced using vegetal lipase microcapsules as a catalyst; when microencapsulated recombinant lipase was used as catalyst, the initial yield could reach 60.5%. After 8 h of reaction, for both biocatalysts, the FAEE yield was greater than 95%. At a longer reaction time than 8 h, the catalytic activity remained steady.
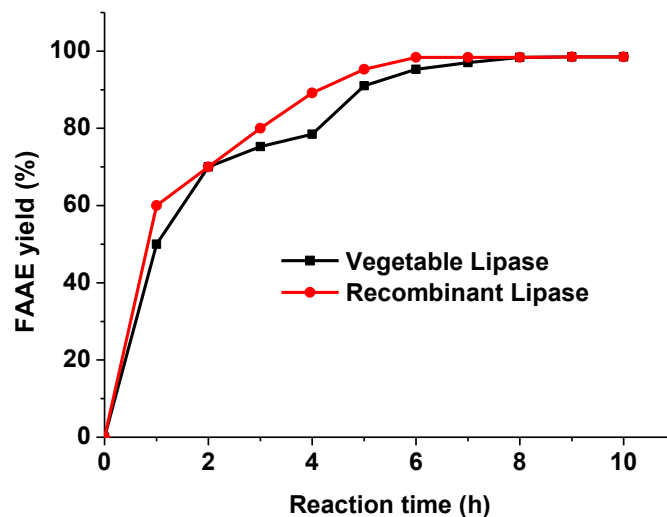

Figure 7. Effect of reaction time on the transesterification of crude *Jatropha curcas* L. oil. Reaction parameters: *Jatropha curcas* L. oil 10 g, ethanol to oil mass ratio 10, water content 9.1 wt%, immobilized lipase 5.25 g, mixing intensity 6 g RCF, temperature 35 °C, pH value 7.5.

3.3.5. Blank Test and Catalyst Reusability

For comparison purposes, the blank experiments including the free lipase and bared microbeads as catalysts were carried out under optimal reaction conditions. The catalytic activity expressed as biodiesel yields were comparatively measured as a reference. The biodiesel yields obtained were 95.2% using *Candida antarctica* (CALb) recombinant *Aspergillus oryzae* and 92.7% using the vegetal of *Jatropha curcas* L. (var. Sevangel) as a catalyst. These two lipases are quite active for the transesterification of *Jatropha curcas* L. oil. It was also found that bared microbeads showed a certain activity for transesterification reaction, leading to approximately 4.6% biodiesel yield as they presented various functional groups such as hydroxyls and carbonyl groups.

The catalyst reusability was evaluated and the results obtained in the consecutive 8 reaction runs are shown in Figure 8. In the first to third reaction runs, both catalysts remained almost unchanged in biodiesel yield. However, from the fourth to eighth reaction runs, approximately a 7.5% decrease in biodiesel yield for the microcapsules carrying on recombinant lipase, and a 10% decrease for the microcapsules carrying on vegetable lipase were observed. Several reasons may be responsible for the gradual drop of catalytic activity: (i) lipase desorption from the microcapsules. During the reaction, mechanical agitation may lead to some lipase removal from the matrix; (ii) water may be stripped by ethanol, diminishing the formation of water-oil micro interfaces, which disfavors the maintenance of the conformation of lipase structure. Our previous study confirms that a step-wise addition of alcohol can reduce this effect as it can inhibit the water stripping by alcohol [43].
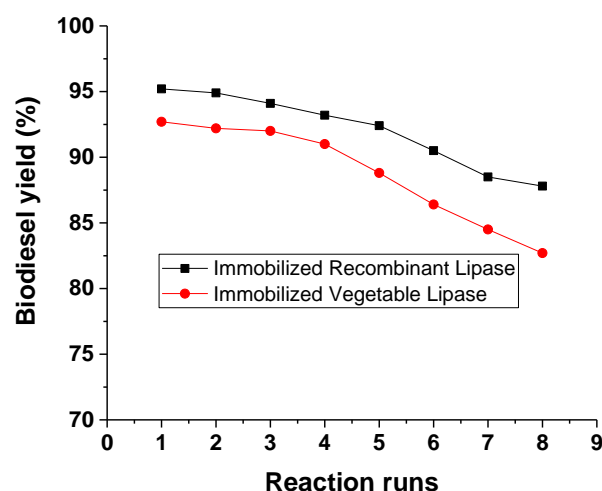
Figure 8. Catalyst reusability evaluation in 8 reaction cycles. Reaction condition: *Jatropha curcas* L. oil 10 g, ethanol-to-oil mass ratio 10, water content 9.1 wt%, immobilized lipase 5.25 g, mixing intensity 6 g RCF, temperature 35° C, pH value 7.5.

3.3.6. Biodiesel Characterization and Quality

The quality of the biodiesel obtained by this research was comparatively analyzed by the FTIR technique with respect to the initial JCLO feedstock and the sample obtained during the reaction process (Figure 9).
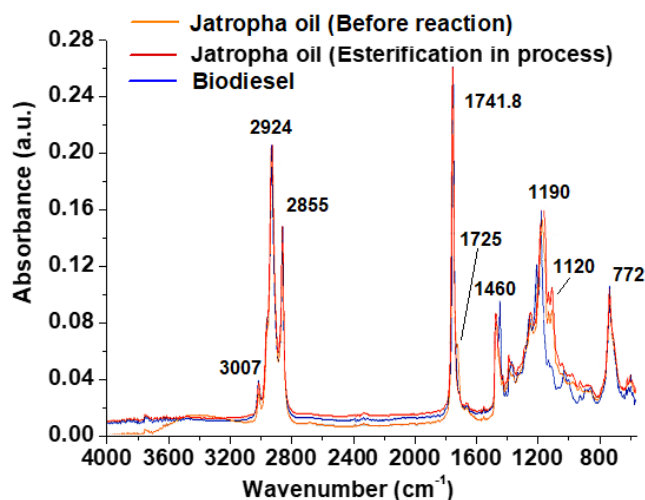

Figure 9. FTIR spectra of the obtained biodiesel, the oil obtained during the transesterification procedure and the JCO procedure.

The sharp band at 1741.8 cm^{-1} was assigned to the characteristic of the axial deformation vibration of the ester double bond C=O [44,45]. The two bands at 1243 and 1190 cm^{-1} correspond to the axial deformations of the C–O bond in an ester [46]. A group of IR bands appeared between 2855 and 3007 cm^{-1} for the biodiesel product and Jatropha oil feedstock. The IR bands at 2924 to 2855 cm^{-1} corresponded to the stretching vibrations of the symmetric and asymmetric C–H bond of the –CH$_3$ and –CH$_2$ methyl groups in the hydrocarbon chains [47]. And the weak signal at 3007 cm^{-1} was the typical stretching vibrations of the =C–H olefinic group as some unsaturated double bonds exist in the hydrocarbon chains before and after the reaction. The IR bands at 1361 and 1460 cm^{-1} were assigned to the extension vibration of –CH$_3$ and –CH$_2$ groups in the hydrocarbon chains [48]. At the low wavenumber region, the band at 772 cm^{-1} was due to the bending vibration of –CH$_2$ in hydrocarbon chains [45]. The IR bands at 772 cm^{-1} and between 2800

and 3100 cm^{-1} are overlapped for both Jatropha and biodiesel, resulting from the similarity of their hydrocarbon chain.

In comparison with the JCLO feedstock, the weak shoulder at 1725 cm^{-1} in the biofuel disappeared, indicating that the functional group of the carboxylic acid head (–COOH) was already replaced by the ester head (–COOC$_2$H$_5$). With respect to the IR spectrum of the obtained biodiesel, the double bands at approximately 1120–1140 cm^{-1} significantly reduced, indicating the elimination of the C–OH group in the carboxylic acid group (–COOH) in JCLO reactant and the addition of –OC$_2$H$_5$ species. These characterization results confirmed the formation of biodiesel after the JCLO transesterification reaction.

The properties of the obtained biodiesel are reported in Table 5. In comparison with the most unsaturated fatty acids such as oleic and linoleic fatty acids in the Jatropha oil, biodiesel showed a relatively low oxidation stability. All the properties of Jatropha biodiesel in the present work satisfied well the standards according to the international biodiesel ASTM D6751 and EN14214 standards.

Table 5. Quality of the biodiesel obtained via transesterification of JCLO using microencapsulated recombinant lipase as biocatalyst.

Parameters	Values
Flash point (°C)	98.00
Absolute viscosity (mPa·s)	10.093
Kinematic viscosity ((mm)^2/s)	11.349
Ethyl ester content (wt%)	97.2
Triglyceride content (wt%)	90.8
Free fatty acids (g/gKOH)	2.17
Acidity index	4.31
Volatiles content (wt%)	0.47
Ethyl esters content (wt%)	96.5
Triglyceride content (wt%)	94.4
Residual carbon content (wt%)	0.63
Ash content (wt%)	0
Oxidation stability (h)	3.66

4. Conclusions

The microencapsulated lipases used as biocatalysts have been possible to synthesize by the dripping and jet break-up technique using an aqueous mixture of sodium alginate and lipase solution. The size of the microcapsules and their hardness depended mainly on the diameter of the outer nozzle, the flow rate of the solution, and the properties of the cross-linking agent. For obtaining spherical microcapsules, a CaCl$_2$ solution (11 g/L) was used as a hardening agent, and the minimum sodium alginate concentration was 15 g/L which corresponded to the critical Oh number 0.24, and the viscosity of the sodium alginate solution must be above a certain value, i.e., 50 mPa.s.

The crude *Jatropha curcas* L. oil from the Tabasco State of Mexico chiefly contained oleic, linoleic, palmitic, and stearic acids with a viscosity ranging from 24.50 to 28.80 cSt, specific density 0.91 g/cm^3, acidity index 0.70 to 0.79 KOHmg/g oil and iodine index between 98.82 and 102.61 g/100 g. The present investigation confirmed that Tabasco crude *Jatropha curcas* L. oil can be directly used as feedstock without pretreatment for the production of biodiesel via the transesterification reaction.

For the production of biodiesel catalyzed with the microencapsulated lipase biocatalysts and JCLO as feedstock, the optimal transesterification reaction parameters were obtained: reaction temperature 35 °C, ethanol-to-oil mass ratio 10, water addition 9.1 wt%, immobilized lipase microcapsules mass 5.25 g, pH value 7.5, relative centrifugal force 6 g, and reaction time 8 h. Under the optimal reaction condition, an approximately 95% fatty acid ethyl esters yield was achieved. The quality of the obtained biodiesel satisfied well with the corresponding standards ASTM D6751 and EN14214. The microencapsulation technique reported herein allows obtaining microcapsules on a large scale with the charac-

teristics required for sustainable biofuel production, which can make the enzymatic process for biodiesel production economically feasible.

Abbreviations

AFM	Atomic force microscopy.
CALb	*Candida antarctica* lipase B.
CIBIOC	Center for Innovation in Inputs for Bioenergetics and Co-Products.
CINVESTAV	Centro de Investigación y de Estudios Avanzados.
CLEAs	Cross-linked enzyme aggregates.
CMP + L	Centro Mexicano para la Producción Más Limpia (Mexican Centre for Cleaner Production).
CONACyT	Consejo Nacional de Ciencias y Tecnología.
ESIQIE	Escuela Superior de Ingeniería Química e Industrias Extractivas (Superior School of Chemical Engineering and Extractive Industries).
FAEEs	Fatty acid ethyl esters.
JCLO	*Jatropha curcas* L. oil.
LaNDACBio	El Laboratorio Nacional de Desarrollo y Aseguramiento de la Calidad en Biocombustibles (National Laboratory for Development and Quality Assurance of Biofuels).
MCs	Microcapsules.
Oh number	Ohnesorge number.
RCF:	Relative centrifugal force.
UCyEH:	Unidad de Caracterización y Evaluación de Hidrocarburos.

References

1. Rahmath, A.; Chan, E.S.; Ravindra, P. Biodiesel production from *Jatropha curcas*: A critical review. *Crit. Rev. Biotechnol.* **2011**, *31*, 53–64. [CrossRef]
2. Koh, M.Y.; Ghazi, T.M. A review of biodiesel production from *Jatropha curcas* L. oil. *Renew Sustain. Ener. Rev.* **2011**, *15*, 2240–2251. [CrossRef]
3. Azam, M.M.; Waris, A.; Nahar, N.M. Prospects and potential of fatty acid methyl esters of some non-traditional seed oils for use as biodiesel in India. *Biomass Bioenergy* **2005**, *29*, 293–302. [CrossRef]
4. Oliveira, J.S.; Leite, P.M.; Souzaa, L.B.; Mello, V.M.; Silva, E.C.; Rubima, J.C.; Meneghetti, S.M.P.; Suarez, P.A.Z. Characteristics and composition of Jatropha gossypiifolia and *Jatropha curcas* L. oils and application for biodiesel production. *Biomass Bioenergy* **2009**, *33*, 449–453. [CrossRef]
5. Achten, W.M.J.; Verchot, L.; Franken, Y.J.; Mathijs, E.; Singh, V.P.; Aerts, R. Jatropha bio-diesel production and use. *Biomass Bioenergy* **2008**, *32*, 1063–1084. [CrossRef]
6. Intarapong, P.; Langthanarat, S.; Phanthong, P.; Luengnaruemitchai, A.; Jai-In, S. Activity and basic properties of KOH/mordenite for transesterification of palm oil. *J. Energy Chem.* **2013**, *22*, 690–700. [CrossRef]

7. Efavi, J.K.; Kanbogtah, D.; Apalangya, V.; Nyankson, E.; Tiburu, E.K.; Dodoo-Arhin, D.; Onwona-Agyeman, B.; Yaya, A. The effect of NaOH catalyst concentration and extraction time on the yield and properties of *Citrullus vulgaris* seed oil as a potential biodiesel feed stock. *S. Afr. J. Chem. Eng.* **2018**, *25*, 98–102. [CrossRef]

8. Aghaei, H.; Yasinian, A.; Taghizadeh, A. Covalent immobilization of lipase from Candida rugosa on epoxy-activated cloisite 30B as a new heterofunctional carrier and its application in the synthesis of banana flavor and production of biodiesel. *Int. J. Biol. Macromol.* **2021**, *178*, 569–579. [CrossRef]

9. Ismail, A.R.; Baek, K.-H. Lipase immobilization with support materials, preparation techniques, and applications: Present and future aspects. *Int. J. Biol. Macromol.* **2020**, *163*, 1624–1639. [CrossRef]

10. Katiyar, M.; Abidam, K.; Ali, A. Candida rugosa lipase immobilization over SBA-15 to prepare solid biocatalyst for cotton seed oil transesterification. *Mater. Today Proc.* **2021**, *36*, 763–768. [CrossRef]

11. Abdulla, R.; Ravindra, P. Characterization of cross linked Burkholderia cepacia lipase in alginate and κ-carrageenan hybrid matrix. *J. Taiwan Inst. Chem. Eng.* **2013**, *44*, 545–551. [CrossRef]

12. Tischer, W.; Wedekind, F. *Immobilized Enzymes: Methods and Applications, Biocatalysis-From Discovery to Application*; Springer: Berlin/Heidelberg, Germany, 1999; pp. 95–126. [CrossRef]

13. Krajewska, B. Application of chitin-and chitosan-based materials for enzyme immobilizations: A review. *Enzyme Microb. Tech.* **2004**, *35*, 126–139. [CrossRef]

14. Shahrampour, D.; Khomeiri, M.; Razavi, S.M.A.; Kashiri, M. Development and characterization of alginate/pectin edible films containing Lactobacillus plantarum KMC 45. *LWT* **2020**, *118*, 108758. [CrossRef]

15. Noureddini, H.; Gao, X.; Philkana, R.S. Immobilized Psuedomonas cepacia lipase for biodiesel fuel production from soybean oil. *Bioresour. Technol.* **2005**, *96*, 769–777. [CrossRef]

16. Triantafyllou, A.O.; Wehtje, E.; Adlercreutz, P.; Mattiasson, B. Effects of sorbitol addition on the action of free and immobilized hydrolytic enzymes in organic media. *Biotechnol. Bioeng.* **1995**, *45*, 406–414. [CrossRef]

17. Sánchez-Bayo, A.; Morales, V.; Rodríguez, R.; Vicente, G.; Bautista, L.F. Biodiesel Production (FAEEs) by Heterogeneous Combi-Lipase Biocatalysts Using Wet Extracted Lipids from Microalgae. *Catalysts* **2019**, *9*, 296. [CrossRef]

18. Betigeri, S.S.; Neau, S.H. Immobilization of lipase using hydrophilic polymers in the form of hydrogel beads. *Biomaterials* **2002**, *23*, 3627–3636. [CrossRef]

19. Badgujar, K.C.; Bhanage, B.M. Enhanced Biocatalytic Activity of Lipase Immobilized on Biodegradable Copolymer of Chitosan and Polyvinyl Alcohol Support for Synthesis of Propionate Ester: Kinetic Approach. *Ind. Eng. Chem. Res.* **2014**, *53*, 18806–18815. [CrossRef]

20. Garg, A.; Chhipa, K.; Kumar, L. Microencapsulation techniques in pharmaceutical formulation. *Eur. J. Pharm. Med. Res.* **2022**, *5*, 199–206.

21. Roshan, K.; Rathore, K.S.; Meenakshi, B.; Amul, M. Microencapsulation drug delivery system—An overview. *Pharma Tutor* **2016**, *4*, 20–28.

22. Chandak, M.P.; Adhao, V.S.; Thenge, R. Microsphere: A novel drug delivery system. *Int. J. Pharm. Technol.* **2020**, *12*, 31955–31973. [CrossRef]

23. Ayoub, A.; Sood, M.; Singh, J.; Bandral, J.D.; Gupta, N.; Bhat, A. Microencapsulation and its applications in food industry. *J. Pharmacogn. Phytochem.* **2019**, *8*, 32–37.

24. Bradford, M.M. A Rapid and Sensitive Method for the Quantitation of Microgram Quantities of Protein Utilizing the Principle of Protein-Dye Binding. *Anal. Biochem.* **1976**, *72*, 248–254. [CrossRef] [PubMed]

25. Lu, J.; Deng, l.; Zhao, R.; Zang, R.; Wang, F.; Tan, T. Pretreatment of immobilized Candida sp. 99-125 lipase to improve its methanol tolerance for biodiesel production. *J. Mol. Catal. B Enzym.* **2010**, *62*, 15–18. [CrossRef]

26. Wyss, A.; von Stockar, U.; Marison, I.W. A novel reactive perstraction system based on liquid-core microcapsules applied to lipase-catalyzed biotransformations. *Biotechnol. Bioeng.* **2006**, *93*, 28–39. [CrossRef] [PubMed]

27. Whelehan, M.; Marison, I.W. Microencapsulation Using Vibrating Technology. *J. Microencapsul.* **2011**, *28*, 669–688. [CrossRef]

28. Foresti, M.L.; Valle, G.; Bonetto, R.; Ferreira, M.L.; Briand, L.E. FTIR, SEM and fractal dimension characterization of lipase B from Candida antarctica immobilized onto titania at selected conditions. *Appl. Surf. Sci.* **2010**, *256*, 1624–1635. [CrossRef]

29. Cruz, M.; Almeida, M.F.; Alvim-Ferraz, M.D.C.; Dias, J.M. Monitoring Enzymatic Hydroesterification of Low-Cost Feedstocks by Fourier Transform InfraRed Spectroscopy. *Catalysts* **2019**, *9*, 535. [CrossRef]

30. Langel, W.; Menken, L. Simulation of the interface between titanium oxide and amino acids in solution by first principles MD. *Surf. Sci.* **2003**, *538*, 1–9. [CrossRef]

31. Silverstein, R.M.; Bassler, G.C.; Morrill, T.C. *Spectrometric Identification of Organic Compounds*; J. Wiley & Sons: New York, NY, USA, 1991.

32. Rabelo, S.N.; Ferraz, V.P.; Oliveira, L.S.; Franca, A.S. FTIR Analysis for quantification of fatty acid methyl esters in biodiesel produced by microwave-assisted transesterification. *Int. J. Environ. Sci. Dev.* **2015**, *6*, 964–969. [CrossRef]

33. Akbar, E.; Yaakob, Z.; Kamarudin, S.T.; Ismail, M.; Salimon, J. Characteristic and composition of *Jatropha curcas* oil seed from Malaysia and its potential as biodiesel feedstock. *Eur. J. Sci. Res.* **2009**, *29*, 396–403.

34. Gopale, K.D.; Zunjarrao, R.S. Variations in Biochemical Content of *Jatropha curcas* Seeds Collected from Agroclimatic Zones of Maharashtra State of India. *IUP J. Life Sci.* **2011**, *5*, 27–38.

35. Martínez, H.J.; Siddhuraju, P.; Francis, G.; Dávila-Ortíz, G.; Becker, K. Chemical composition, toxic/antimetabolic constituents, and effect of different treatments on their levels, in four provenances of *Jatropha curcas* from México. *Food Chem.* **2006**, *96*, 80–89. [CrossRef]

36. Antczak, S.M.; Kubiak, A.; Antczak, T.; Bielecki, S. Enzymatic biodiesel synthesis—Key factors affecting efficiency of the process. *Renew. Energy* **2009**, *34*, 1185–1194. [CrossRef]

37. Fernandez-Lorente, G.; Palomo, J.M.; Guisan, J.M.; Fernandez-Lafuente, R. Effect of the immobilization protocol in the activity, stability, and enantioslectivity of Lecitase® Ultra. *J. Mol. Catal. B Enzym.* **2007**, *47*, 99–104. [CrossRef]

38. Kaieda, M.; Samukawa, T.; Kondo, A.; Fukuda, H. Effect of methanol and water contents on production of biodiesel fuel from plant oil catalyzed by various lipases in a solvent-free system. *J. Biosci. Bioeng.* **2001**, *91*, 12–15. [CrossRef]

39. Kumari, V.; Shweta, S.; Munishwar, N. Preparation of biodiesel by lipase-catalyzed transesterification of high free fatty acid containing oil from *Madhuca indica*. *Energ. Fuels* **2007**, *21*, 368–372. [CrossRef]

40. Li, X.; Xu, H. Large-scale biodiesel production from microalga Chlorella protothecoides through heterotrophic cultivation in bioreactors. *Biotechnol. Bioeng.* **2007**, *98*, 764–771. [CrossRef]

41. Puthli, M.S.; Rathod, V.K.; Pandit, A.B. Enzymatic hydrolysis of castor oil: Process intensification studies. *Biochem. Eng. J.* **2006**, *31*, 31–41. [CrossRef]

42. Ogunniyi, D.S. Castor Oil: A vital industrial raw material. *Bioresour. Technol.* **2006**, *97*, 1086–1091. [CrossRef]

43. Méndez, J.C.; Arellano, U.; Solís, S.; Wang, J.A.; Chen, L.F. Synthesis and catalytic activity of lipase immobilized Ca/Kit-6 biocatalysts for transesterification of coconut oil to biodiesel. *Mol. Catal.* **2022**, *533*, 112793. [CrossRef]

44. Shapaval, V.; Brandenburg, J.; Blomqvist, J.; Tafintseva, V.; Passoth, V.; Sandgren, M.; Kohler, A. Biochemical profiling, prediction of total lipid content and fatty acid profile in oleaginous yeasts by FTIR spectroscopy. *Biotechnol. Biofuels* **2019**, *12*, 140. [CrossRef] [PubMed]

45. Núñez, F.; Chen, L.F.; Wang, J.A.; Flores, S.O.; Salmones, J.; Arellano, U.; Tzompantzi, F.; Noreña, L.E. Bifunctional Co_3O_4/ZSM-5 mesoporous catalysts for the production of biodiesel via esterification of oleic acid with methanol. *Catalysts* **2022**, *12*, 900. [CrossRef]

46. Patel, A.; Narkhede, N. Biodiesel synthesis via esterification and transesterification over a new heterogeneous catalyst comprising lacunary silicotungstate and MCM-41. *Catal. Sci. Technol.* **2013**, *3*, 3317–3325. [CrossRef]

47. De Lira, L.; De Vasconcelos, F.; Pereira, C.F.; Silveira, A.; Stragevitch, L.; Pimentel, M. Prediction of properties of diesel/biodiesel blends by infrared spectroscopy and multivariate calibration. *Fuel* **2010**, *89*, 405–409. [CrossRef]

48. Samanta, S.; Sahoo, R.R. Waste Cooking (Palm) Oil as an Economical Source of Biodiesel Production for Alternative Green Fuel and Efficient Lubricant. *Bioenergy Res.* **2021**, *14*, 163–174. [CrossRef]